Limited exchange between the deep Pacific and Atlantic oceans during the warm mid-Pliocene and MIS M2 "glaciation"

Anna Hauge Braaten[1], Kim A. Jakob[2], Sze Ling Ho[1,3], Oliver Friedrich[2], Eirik Vinje Galaasen[1], Stijn De Schepper[4], Paul A. Wilson[5] and Anna Nele Meckler[1,]

[1]Department of Earth Science and Bjerknes Centre for Climate Research, University of Bergen, Bergen, 5007, Norway
[2]Institute of Earth Sciences, Heidelberg University, Heidelberg, 69120, Germany
[3]Institute of Oceanography, National Taiwan University, Taipei, 10617, Taiwan
[4]NORCE Norwegian Research Centre and Bjerknes Centre for Climate Research, Bergen, 5007, Norway
[5]University of Southampton, Waterfront Campus, National Oceanography Centre, Southampton, SO14 3ZH, UK

Correspondence to: Anna H. Braaten (anna.braaten@uib.no)

Abstract

The Piacenzian stage (3.6–2.6 Ma) of the Pliocene is the most recent period where Earth experienced sustained intervals of global warmth analogous to predicted near-future climates. Despite considerable efforts to characterize and understand the climate dynamics of the Piacenzian, the deep ocean and its response to this warming remains poorly understood. Here we present new mid-Piacenzian Mg/Ca and Δ_{47} ("clumped isotope") temperatures from the deep Pacific and North Atlantic oceans. These records cover the transition from Marine Isotope Stage (MIS) M2 — considered the most pronounced "glacial" stage of the Pliocene prior to the intensification of Northern Hemisphere glaciaion — to the warm KM5 interglacial. We find that a large (>4°C) temperature gradient existed between these two basins throughout that interval, with the deep North Atlantic considerably warmer and likely saltier than at present. We interpret our results to indicate that the deep Pacific and North Atlantic oceans were bathed by water masses with very different physical properties during the mid-Piacenzian, and that only limited deep oceanic exchange occurred between the two basins. Our results point to a fundamentally different mode of ocean circulation or mixing compared to the present, where heat and salt is distributed from the North Atlantic into the Pacific. The amplitude of cooling observed at both sites during MIS M2 suggests that changes in benthic $\delta^{18}O$ associated with this cold stage were mostly driven by temperature change in the deep ocean rather than ice volume.

1 Introduction

Our ability to predict future climate change in response to anthropogenic CO_2 emissions partially rests on our understanding of how the climate system has operated under similar conditions in the past. The Piacenzian stage of the Pliocene (3.6–2.6 million years ago, Ma) is the most recent interval in the geological past with sustained intervals of global warmth. The mid-Piacenzian warm period (mPWP, 3.264–3.025 Ma) in particular, has received considerable attention as a useful point of

1

comparison for near-future climates (e.g. Burke et al., 2018). At this time, atmospheric CO_2 concentrations were comparable to the present (~350–450 ppm, de la Vega et al., 2020 and references therein) and many important tectonic and geographical boundary conditions were similar to today.

Considerable efforts have been made to characterize and understand the climate dynamics of the mPWP. Globally averaged surface temperatures were elevated by ~2–3 °C relative to the pre-industrial (McClymont et al., 2020; Haywood et al., 2020), with much of that warming concentrated in the high latitudes. Meanwhile, maximum temperatures in the tropical warm pools appear to have been comparable to today (~29 °C) (Wara et al., 2005; Meinicke et al., 2021), resulting in significantly reduced meridional temperature gradients. Sea-level rise of the magnitude proposed for the mPWP (~20 meters above present) (Dwyer and Chandler, 2009; Rohling et al., 2014; Grant et al., 2019; Dumitru et al., 2019) would require reduced ice sheet extent in both hemispheres. In equilibrium with CO_2 concentrations comparable to the early 21th Century, it appears that the climate of the mid-Piacenzian was warm enough to prevent growth of significant continental ice in the Northern Hemisphere (Dumitru et al., 2019).

Earth system models have largely been unable to simulate the full magnitude of Arctic amplification and reduced meridional temperature gradients implied by proxy reconstructions (Dowsett et al., 2012; Salzmann et al., 2013; de Nooijer et al., 2020), suggesting that key feedback mechanisms for the mPWP may be underestimated or missing in these models. Increased poleward heat transport, decreased ice-albedo and feedbacks related to cloud-cover are some of the mechanisms proposed to have contributed to Pliocene warmth (Fedorov et al., 2006), but a full understanding of the processes that caused and maintained these conditions is still missing.

While climatic conditions of the Piacenzian were typically warm, this stage also contains distinct climate variability. Most notably, it includes a short-lived but pronounced "glacial" event during Marine Isotope Stage (MIS) M2 (3.312–3.264 Ma) immediately prior to the mPWP. MIS M2 is the largest positive benthic oxygen isotope excursion (~0.6 ‰) in the Pliocene prior to the intensification of Northern Hemisphere glaciation (iNHG) (Lisiecki and Raymo, 2005), and has been suggested to represent an early, "failed attempt" at establishing a pattern of Northern Hemisphere glacial-interglacial cycles (Haug and Tiedemann, 1998). Estimates of sea-level fall associated with this event vary greatly, ranging from ~10 to 65 meters below present level (Dwyer and Chandler, 2009; Naish and Wilson, 2009; Miller et al., 2012). To what extent the oxygen isotope event reflects ice growth on land versus cooling of the deep ocean, however, remains a topic of debate.

The deep ocean plays an integral role in modulating climate on long and short timescales, acting as a major reservoir for heat and CO_2 that responds to and affects surface conditions. Although the Pliocene deep ocean remains poorly characterized, with available temperature records sparse and occasionally contradictory, existing reconstructions suggest the deep ocean could have operated differently than today. In the North Atlantic, available data suggest average mPWP bottom water temperatures

Deleted: is the mid-Pliocene (3.3–3.0 million years ago, Ma), when…

Deleted: was

Deleted: values

Deleted: mid-Pliocene

Deleted: mid-Pliocene

Deleted: Pliocene

Deleted: mid-Pliocene

Deleted: mid-Pliocene

Deleted: interval

Deleted:).

Deleted: mid-

(BWTs) were either similar to today (Dwyer et al., 1995; Cronin et al., 2005; Dwyer and Chandler, 2009) or significantly warmer (Bartoli et al., 2005; Sosdian and Rosenthal, 2009). The deep North Pacific, however, may have been — on average — colder than today during the mPWP (Woodard et al., 2014). Based on comparison of this North Pacific record (Site 1208, 3346 meters water depth) with North Atlantic BWTs from Site 607 (3426 meters water depth, Sosdian and Rosenthal, 2009), Woodard et al. (2014) conclude that a large bottom water temperature gradient of up to 4 °C existed between the two basins in the Pliocene prior to the iNHG at ~2.7 Ma. In comparison, the modern deep ocean is relatively isothermal across the various basins, with only a ~1°C difference between the deep (>3000 meters) Atlantic, Pacific and Indian Oceans (Locarnini et al., 2013) (Fig. 1). The existence of a strong temperature gradient in the Pliocene would have important implications for characterising ocean circulation and global climate, determining for example where heat resided in the climate system and the route and efficiency of heat transport. A growing number of studies have suggested that the North Pacific Ocean was a site of deep convection and deep water formation (North Pacific Deep Water, NPDW) (Burls et al., 2017; Shankle et al., 2021; Ford et al., 2022) in the warm Pliocene. If true, this would leave open the possibility that the records of Woodard et al. (2014) from Shatsky Rise, which suggest colder-than-present temperatures during the mPWP, are recording a local North Pacific signal rather than representing the deep Pacific as a whole.
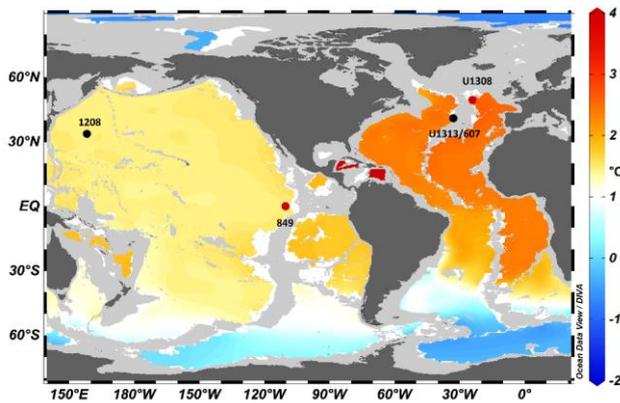
Figure 1. Modern water temperatures at 3800 meters water depth with locations of sites used (in red) and referenced (in black). Temperature data from the World Ocean Atlas 2013 (Locarnini et al., 2013). Map generated in Ocean Data View (ODV 5.6.3, Schlitzer, 2023)

Available BWT records from the mid-Piacenzian have exclusively been based on Mg/Ca thermometry. The Mg/Ca paleothermometer is influenced by a number of non-thermal effects that complicate the application this proxy, which could explain some of the discrepancies observed between various Pliocene BWT records. Mg/Ca ratios of epifaunal benthic

3

foraminifera can be affected by changes in carbonate ion saturation state (Elderfield et al., 2006; Lear et al., 2010), and it has been suggested that the North Atlantic Mg/Ca-based temperature record by Sosdian and Rosenthal (2009) was compromised by such effects (Yu and Broecker, 2010). Additionally, strong vital effects have been documented in foraminifera — making species-specific calibrations necessary (i.e. Lear et al., 2002), and some of the Mg/Ca-based estimates are from ostracods, possibly explaining discrepancies from foraminiferal records. Furthermore, seawater Mg/Ca (Mg/Ca_{sw}), while globally uniform at any given time, changes on geological timescales (e.g. Wilkinson and Algeo, 1989; Dickson, 2004; Coggon et al., 2010). Adjustments for this change on long time scales have been applied since the first applications of the Mg/Ca BWT proxy (Lear et al., 2000), but estimates of the magnitude of change — and thus its effect on reconstructed temperatures — varies between studies (Evans et al., 2016; Tierney et al., 2019).

A novel approach for estimating BWTs in the Pliocene is carbonate clumped isotope (Δ_{47}) thermometry of benthic foraminifera. This paleothermometer is based on the thermodynamic preference for rare, heavy isotopes to bond within the same carbonate ion with decreasing temperatures, and involves measuring the excess abundance of ^{13}C-^{18}O bonds relative to their stochastic abundance (Ghosh et al., 2006; Schauble et al., 2006). This proxy produces temperature estimates that are independent of the chemical composition of the parent water (e.g. Eiler, 2011), making it a particularly powerful tool for reconstructing ocean temperatures in environments where the composition of seawater cannot be well constrained. Furthermore, no detectable species-specific vital effects have been found for benthic foraminifera (Tripati et al., 2010; Peral et al., 2018; Piasecki et al., 2019). While Δ_{47} is a highly useful proxy for reconstructing absolute temperatures, the large quantities of carbonate sample material required for reliable temperatures coupled with the large analytical uncertainties and time-intensive nature of the measurements, makes it less suited for high-resolution work.

To address the discrepancies between currently available deep-sea temperature records for the mid-Piacenzian and assess the existence of a large temperature gradient between the Pacific and Atlantic basins we present new paired benthic foraminiferal Mg/Ca and Δ_{47} temperatures from Ocean Drilling Program (ODP) Site 849 in the deep Equatorial East Pacific and Integrated Ocean Drilling Program (IODP) Site U1308 in the deep North Atlantic. The records cover the interval from Marine Isotope Stage (MIS) M2 — considered the most pronounced "glacial" stage of the Pliocene prior to iNHG — to the warm interglacial MIS KM5c, which has a near identical orbital configuration to the present and thus possibly offers the best analogue for our current climate (i.e. Haywood et al., 2013). This allows us to not only compare mean deep-sea temperatures in the Pacific and Atlantic basins, but also to investigate the variability over key warming and cooling stages of the Piacenzian. Because Mg/Ca records at both sites were generated on the same shallow-infaunal benthic foraminiferal species (*Oridorsalis umbonatus*), and samples and data were treated identically, the records are more directly comparable than those of previous studies. Δ_{47} temperatures measured on the same samples provide an independent check on absolute Mg/Ca temperatures, bypassing uncertainties related to seawater chemistry or species effects. In combination, the two proxies provide robust constraints on

4

bottom-water temperatures in the deep Pacific and North Atlantic for the mid-Piacenzian and allows us to examine if changes

155 in benthic δ^{18}O associated with MIS M2 are caused by temperature or ice volume.

2 Materials and Methods

2.1 Materials, site locations and sample processing

2.1.1 ODP Site 849

ODP Site 849 is situated on the western flank of the East Pacific Rise (Fig. 1) (0°11'N, 110°31'W) at a water depth of 3851

160 meters (Mayer et al., 1992). It is today bathed by Pacific Deep Water (PDW), a water mass largely consisting of Antarctic Bottom Water (AABW), with smaller contributions from Antarctic Intermediate Water (AAIW) and recirculated North Atlantic Deep Water (NADW) (Mix et al., 1995; Kwiek and Ravelo, 1999). This study site was chosen as it is considered to approximate mean deep Pacific conditions, and is suggested to have been permanently bathed by Southern Component Waters (SCW) throughout the Plio-Pleistocene (Mix et al., 1995). Although the present day water depth at Site 849 sits below the

165 modern eastern equatorial lysocline at ~3400 (Berger et al., 1982) the site has remained above the carbonate compensation depth for the past 34 Ma (Pälike et al., 2012). Previous studies have concluded that this site exhibits good foraminiferal test preservation, excellent age control and high sedimentation rates across our study interval (Jakob et al., 2021a, Jakob et al., 2021b, see also Fig. S1). We investigated samples along the primary shipboard splice, from cores 849D-8H-5-6 cm to 849D-8H-6-96 cm and 849C-9H-1-46 cm to 849C-9H-3-18 cm (87.67–92.77 meters composite depth, mcd), corresponding to 3.160–

170 3.334 Ma on the updated age model of Jakob et al. (2021b). A total of 248 (20 cm³) samples were collected at 2-cm intervals, and the material was dried, weighed and washed over a 63 μm sieve. Tests of the benthic foraminifer *O. umbonatus* were picked from the >150 μm dried sediment fraction for Mg/Ca analysis. In addition, remaining benthic foraminifera were picked from selected samples (n=44, >150 μm fraction) for clumped isotope analysis.

2.1.2 IODP Site U1308

175 IODP Site U1308 constitutes a reoccupation of Deep Sea Drilling Project (DSDP) Site 609, a benchmark location for late Pleistocene North Atlantic climate records. Site U1308 is situated on the eastern flank of the Mid-Atlantic Ridge (Fig. 1) (49°52'N, 24°14'W) at a water depth of 3871 meters (Expedition 303 Scientists, 2006). Today, this site is bathed by Lower North Atlantic Deep Water (LNADW) and Lower Deep Water (LDW), with LDW consisting of a mixture of 70–80 % NADW and 20–30% AABW (Arhan et al., 2003). Site U1308 was chosen as it is situated at the same depth as our Pacific site and

180 exhibits good foraminiferal test preservation for our target interval (see suppl. information and Fig. S2).

5

We investigated samples from cores U1308C-25H-5-80 cm to U1308C-26H-6-71.5 cm (253.81–264.71 mcd). Very little work has been done on this portion of the sequence because it falls below the primary shipboard splice (0–248 mcd, ~0–3.1 Ma). However, an age model and benthic foraminiferal (*Cibicidoides wuellerstorfi* and *Uvigerina peregrina*) stable isotope data are available for a short interval from 258.95–264.71 mcd, corresponding to MIS M2 (De Schepper et al., 2013). To extend this record, 53 (20 cm^3) samples were collected at 10 cm spacing from 253.81–259.01 mcd. The new samples were dried, weighed and washed over a 63 μm sieve. The >150 μm sediment fraction of each of these samples was picked for *O. umbonatus* and *C. wuellerstorfi*/*Cibicidoides mundulus* for Mg/Ca and stable isotope analysis, respectively. The interval from 258.95–264.71 mcd was sampled by De Schepper et al. (2013) at a higher resolution, on average every 5 cm (n=113). These samples were picked for *O. umbonatus* for Mg/Ca analysis. Furthermore, remaining benthic foraminifera were picked from 34 samples (>150 μm) across the full study interval for clumped isotope analysis.

2.2 Methods

2.2.1 Stable isotope analysis and age model for Site U1308

Stable isotope ($\delta^{18}O$ and $\delta^{13}C$) analyses were performed on both *C. wuellerstorfi* and *C. mundulus*, as neither species was present continuously throughout the entire study interval. Prior to analysis, foraminiferal tests were ultrasonicated in methanol for 15 seconds to remove fine-grained particles. Analyses were carried out at the Facility for Advanced Isotopic Research and Monitoring of Weather, Climate and Biogeochemical Cycling (FARLAB), Department of Earth Science, University of Bergen, using a Finnigan MAT 253 mass spectrometer coupled to a Kiel IV carbonate device. Measurements were performed on 1–3 tests and replicated two or more times when abundances allowed (~76% of the 47 samples measured). Six samples did not contain enough material for analysis. The long-term reproducibility (1σ) of the in-house working standard (CM12, Carrara marble) during the analysis window was 0.03‰ and 0.06‰ for $\delta^{13}C$ and $\delta^{18}O$, respectively. Results are reported relative to Vienna Pee Dee Belemnite (VPDB), calibrated using National Bureau of Standards (NBS)-19 and crosschecked with NBS-18. We detect no systematic variations in oxygen isotopic offsets between the two species and present the data as an averaged composite record. An apparent inter-lab offset between previously the published benthic foraminiferal $\delta^{18}O$ ($\delta^{18}O_b$) of De Schepper et al. (2013) and our new record was observed. We adjust for this offset by adding 0.29‰ to the values reported in De Schepper et al. (2013) (see supplementary information and Fig. S3 for details).

For Site U1308, a continuation of the existing age model by De Schepper et al. (2013) was established for the interval from 253.81–258.95 mcd by tuning our new $\delta^{18}O_b$ record to the LR04 benthic foraminiferal oxygen isotope stack (Lisiecki and Raymo, 2005) using the software program QAnalySeries 1.5.0.(Kotov and Pälike, 2018). Minor adjustments were also made to the existing age model between 258.95–264.71 mcd. The updated tie-points used for the age model are presented in Table 1.

Deleted: materials

Deleted: S1

Moved down [1]

Table 1. Tie-points used for the updated age model of IODP U1308

Depth (mcd)	Age (Ma)
254.66	3.207
256.77	3.240
261.11	3.284
262.35	3.302
263.25	3.320
263.38	3.327
264.70	3.340

230 **2.2.2 Mg/Ca temperatures**

The benthic foraminiferal species *O. umbonatus* was used for Mg/Ca analysis at both sites. This species was selected because i) it is well buffered against the influence of changes in deep ocean carbonate ion/pH due to its shallow-infaunal habitat (Rathmann and Kuhnert, 2008; Lear et al., 2015), ii) it contains large chambers that can be thoroughly cleaned for Mg/Ca analysis, and iii) it exhibits low sensitivity to temporal variations in the Mg/Ca of seawater (Lear et al., 2015). Furthermore,

235 core top measurements of this species from Site 849 (Jakob et al., 2021a) and North Atlantic Site U1313 (Jakob et al., 2020 suppl. information), have produced Mg/Ca temperatures that are indistinguishable from modern BWTs at the respective sites. These core top studies treated materials identically to our Pliocene samples.

Foraminiferal tests were cracked, homogenized and cleaned following the cleaning protocol of Barker et al. (2003) with the

240 reductive cleaning step omitted to avoid decreasing their Mg/Ca ratios (Barker et al., 2003; Rosenthal et al., 2004). Samples were measured using an Agilent Inductively Coupled Plasma-Optical Emission Spectrometer (ICP-OES) 720 at the Institute of Earth Sciences, Heidelberg University. Reported Mg/Ca values have been normalized relative to the ECRM 751-1 standard (Greaves et al., 2008). Fe/Ca and Mn/Ca ratios were screened to identify potential contamination from clays or coatings that were not removed in the cleaning process (see suppl. information and Fig. S4–S5 for details). Fe/Ca and Mn/Ca ratios were

245 not normalized as the Fe and Mn concentrations of the ECRM standard typically were below the detection limit of the ICP-OES. The ECRM standard was measured at least every 20th sample to monitor instrumental precision. Based on these replicate measurements, the standard deviation for Mg/Ca is ± 0.02 mmol/mol and ± 0.03 mmol/mol for Site 849 and Site U1308 samples, respectively.

Deleted: mid-

255 Bottom water temperatures were calculated using the *O. umbonatus*-specific calibration by Lear et al. (2002):

$$T = \left[\ln \frac{Mg/Ca}{1.008}\right] \times \left[\frac{1}{0.114}\right] \tag{1}$$

This calibration is based on multiple, globally distributed core tops, making it applicable to both study sites. Furthermore, the
260 calibration temperature range of 0.8–9.9 °C covers the temperature range we expect to find in the mid-Pliocene deep ocean. Because this calibration was based on data from materials cleaned following a procedure that includes a reductive step, measured Mg/Ca was adjusted downwards by 10% to account for this difference (Barker et al., 2003; Ford et al., 2016). Values were also adjusted to account for past variation in Mg/Ca$_{sw}$ following Lear et al. (2002) using estimates of past Mg/Ca$_{sw}$ from Evans et al. (2016). Uncertainties associated with our Mg/Ca-based BWT record were calculated using the Paleo-Seawater
265 Uncertainty Solver (PSU Solver) MATLAB script of Thirumalai et al. (2016).

2.2.3 Δ$_{47}$ temperatures

Before clumped isotope (Δ$_{47}$) analysis, foraminiferal tests were carefully cracked open to expose the inside of individual chambers. The broken open tests were ultrasonicated for 10 s in DI water, then 10 s in methanol, followed by another two
270 ultrasonication steps with DI water. Samples were rinsed with DI water after each ultrasonication. Cleaned samples were oven-dried at 50°C until any remaining water was fully evaporated. Scanning electron microscope (SEM) images (Fig. S1 and S2) were taken from a random selection of cleaned samples to verify i) that cleaning had fully removed potential contaminants and ii) that tests were well-preserved (see suppl. information).

275 Clumped isotope measurements were performed using two different Thermo Scientific MAT 253Plus mass spectrometers coupled to Kiel IV carbonate devices, located at FARLAB, Department of Earth Science, University of Bergen. The analytical approach is described in detail by Meckler et al. (2014), Piasecki et al. (2019) and Meinicke et al. (2020). To remove potential organic contaminants, the Kiel devices were equipped with PoraPak traps which were held at -20°C during runs. The traps were baked at 150°C for at least one hour between runs for cleaning. A mix of samples and carbonate standards
280 in a roughly 1:1 ratio was measured in each analytical run. Micro-volume aliquots (70-100 µg) were individually reacted with phosphoric acid (at 70°C) in the Kiel device, and the resulting gas was subsequently measured using the long-integration dual-inlet method (LIDI, Hu et al. 2014) for a total of 400 s. Raw data were corrected for pressure baseline effects based on five daily peak scans (5–25 V, Meckler et al. 2014). Using carbonate standards ETH 1–3, the data were further corrected for scale compression and transferred to the I-CDES scale (Bernasconi et al., 2021). Standard data from the same and adjacent days

Deleted: Error propagation including both analytical and calibration uncertainty produces an error associated with our Mg/Ca-based BWT record of ± 0.9 °C and ± 1.5 °C for Site 849 and U1308 samples, respectively.

Deleted: S4

Deleted: S5

Deleted: .

8

were used for data correction, using a moving window approach. All data correction was done using the Easotope software package (John and Bowen, 2016).

295   Due to the large analytical uncertainty associated with individual Δ_{47} measurements, extensive replication (preferably a minimum of 25–30 measurements) is required to produce reliable temperatures. A large number of benthic foraminiferal species were used to obtain sufficient amounts of sample material (2–4 mg) needed per Δ_{47} temperature. Whenever possible, measurements were performed on aliquots of species- or genus-specific materials. Replicate measurements (n=23–40) from 2–9 adjacent samples were combined to produce each data point. Temperatures were calculated from these averaged Δ_{47} values

300   using the combined foraminifera-based calibration by Meinicke et al. (2020), updated to the I-CDES scale by Meinicke et al. (2021):

$$T = \sqrt{\frac{0.0397 \times 10^6}{\Delta^{47} - 0.1518}} - 273.15 \qquad (2)$$

305   With temperatures given in °C.

The combined analytical and calibration uncertainty was calculated using a Monte Carlo approach (5000 iterations) that samples a random slope-intercept pair for the calibration and a random Δ_{47} value generated from the analytical error and is expressed as 95% confidence intervals on the average temperatures.

310   **2.2.4 Seawater $\delta^{18}O$**

Seawater $\delta^{18}O$ ($\delta^{18}O_{sw}$) was calculated from $\delta^{18}O_b$ in combination with the BWT from Mg/Ca using the *Cibicidoides* and *Planulina* compilation (Eq. 9) from Marchitto et al. (2014):

$$\delta^{18}O_{sw} = [0.245 \times T] - [0.0011 \times T^2] + \delta^{18}O_b - 3.31 \qquad (3)$$

315

Due to the good agreement between the absolute temperatures suggested by the two proxies at both sites (see results), we calculate $\delta^{18}O_{sw}$ from BWT estimates from Mg/Ca, not Δ_{47}, as i) the Mg/Ca records are of significantly higher resolution and ii) the propagated (2σ) uncertainties associated with individual Mg/Ca measurements (±1.2°C and ±1.5°C for 849 and U1308 samples respectively) are smaller than those for the Δ_{47}-based temperature estimates (average of ±2.7°C at both sites). For

320    $\delta^{18}O_{sw}$ calculation we use the published $\delta^{18}O_b$ from Jakob et al. (2021b, generated on *O. umbonatus*) for Site 849 and for Site U1308 the combined record from this study (*C. wuellerstorfi* and *C. mundulus)* and De Schepper et al. (2013) (*C. wuellerstorfi* and *Uvigerina peregrina*), with a +0.29‰ correction of values from the latter (see suppl. Information). To account for species-specific offsets, we normalize measured $\delta^{18}O_b$ of *O. umbonatus* and *Uvigerina spp.* to *Cibicidoides* by subtracting 0.64‰ (Shackleton et al., 1984), allowing us to apply Eq. 3 to all samples.

9

Deleted: 0.8

3 Results

3.1 Pacific Site 849

A total of 233 Mg/Ca measurements were carried out for the interval 3.334–3.160 Ma, yielding a mean temporal resolution of 800 yr. The five-point moving average of Mg/Ca-based BWTs ranges between -0.3°C and 4.6°C (Fig. 2b) while individual values vary from -1.3°C to 6.9°C. The average uncertainty (2σ) associated with the Mg/Ca-based temperatures is ±1.2°C. The equation used to calculate these temperatures has a calibration range of 0.8–9.9 °C (Lear et al., 2002). In total, 42 (~5%) of our measurements fall below this range (-1.3–0.8°C) and are therefore associated with greater uncertainty than the remainder of the record. However, the same would also be true for all other currently available *O. umbonatus*-specific Mg/Ca calibrations (see Jakob et al., 2021a and references therein for a review).

The average Mg/Ca-based temperature over the study interval is ~2.5±1.2°, ~1°C warmer than present BWT at this site (1.6°C, Locarnini et al., 2013) but large changes in BWT are observed throughout the record. Peak temperatures (>4°C) are recorded during all the studied interglacial (as defined from $\delta^{18}O_b$) Marine Isotope Stages (MG1, M1, KM5 and KM3). We observe strong cooling (by ~4°C) associated with the large positive $\delta^{18}O_b$ excursion during MIS M2, although the cooling appears significantly delayed relative to the signal in $\delta^{18}O_b$. Cooling of similar amplitude is also recorded for KM6 and KM4, Marine Isotope Stages not appearing as pronounced glacial stages in benthic oxygen isotope records (Fig. 2a and b).

Ten clumped isotope temperatures were generated over the interval from 3.328–3.189 Ma (Fig. 2b), with each data point representing an average over 23–40 replicate measurements from 2–9 adjacent samples (time interval spanned indicated by horizontal bars in Fig. 2b). Δ_{47}-based BWTs range from 0.7±1.9°C to 5.4±2.3°C (95% CI). The average Δ_{47}-based BWT over the studied interval is 3.5±0.8°C.

Our calculated $\delta^{18}O_{sw}$ record (Fig. 2e) indicates an average value of ~0.0±0.3‰ (2σ) (present bottom water $\delta^{18}O_{sw}$ at Site 849: -0.05‰, LeGrande and Schmidt, 2006) over the study interval. Although $\delta^{18}O_{sw}$ is variable, there is a clear trend of decreasing values over the record — values are higher before and during MIS M2 than afterwards. Average $\delta^{18}O_{sw}$ from 3.334–3.264 Ma (MIS M2 and MG1) is ~+0.3‰. Between 3.263 and 3.160 Ma (MIS M1–KM3), the average $\delta^{18}O_{sw}$ is ~-0.1‰.

Figure 2. Climate indicators and results from Pacific ODP Site 849. All horizontal stippled lines indicate modern values (CO_2 = 2022). (a) Benthic foraminiferal $\delta^{18}O$ from Site 849 (Jakob et al. 2021b, shown with 5pt running mean) and global benthic foraminiferal $\delta^{18}O$ stack (Lisiecki and Raymo, 2005). (b) 849 temperature records. Mg/Ca temperatures shown with 5pt running mean. Horizontal error bars on Δ_{47} temperatures indicate the age range of all individual samples used for each data point. Temperature uncertainties are expressed as solid (68% CI) and stippled (95% CI) bars. (c) Interpolated 1 ka resolution $\delta^{11}B$-derived CO_2 estimates from

11

Figure 2. Climate indicators and results from Pacific ODP Site 849. All horizontal stippled lines indicate modern values ($CO_2 =$ 2022). (a) Benthic foraminiferal $\delta^{18}O$ from Site 849 (Jakob et al. 2021b, shown with 5pt running mean) and global benthic foraminiferal $\delta^{18}O$ stack (Lisiecki and Raymo, 2005). (b) 849 temperature records. Mg/Ca temperatures shown with 5pt running mean. Horizontal error bars on Δ_{47} temperatures indicate the age range of all individual samples used for each data point. Temperature uncertainties are expressed as solid (68% CI) and stippled (95% CI) bars. (c) Interpolated 1 ka resolution $\delta^{11}B$-derived CO_2 estimates from de la Vega et al. (2020). Confidence intervals expressed as dark (68%) and light (95%) shading. (d) Summer insolation forcing at 65°N and 65°S (Laskar et al., 2004). (e) calculated $\delta^{18}O_{sw}$, shown with a linear regression to highlight the overall trend (shading = 95% CI). Note arrows indicating the temporal offsets in the increase in $\delta^{18}O_b$ and decrease in temperature and CO_2. Shaded envelopes on Mg/Ca temperatures and $\delta^{18}O_{sw}$ represent 2σ uncertainties modelled with PSU solver (Thirumalai et al., 2016).

3.2 North Atlantic Site U1308

A total of 49 Mg/Ca measurements were performed for the interval ~3.334–3.196 Ma, yielding a mean temporal resolution of ~3 kyr. The three-point smoothed average of Mg/Ca-based bottom-water temperatures ranges from 5.3–9.3°C, with individual values between 4.5–11.7°C (Fig. 3b). The average uncertainty (2σ) associated with the Mg/Ca-based temperatures is ±1.5°C. A single measurement (11.7°C) falls outside the calibration temperature range of 0.8–9.9°C. The average BWT across the study interval is ~7.2±1.5°C, approximately 4.5°C warmer than the present BWT at this site (2.6°C, Locarnini et al., 2013). The coldest temperatures of the record are reached during MIS M2, but similar temperatures are also reconstructed for MIS KM6. However, the temporal resolution across the most intense $\delta^{18}O_b$ excursion of MIS M2 is low, and our record may underestimate the temperature change associated with this event.

Eight clumped isotope temperatures were generated for the interval from 3.335–3.199 Ma (Fig. 3b), each calculated from an average of 27–34 replicate measurements from 2–7 neighboring samples. Δ_{47}-based BWTs range from 5.6±2.7°C to 10.5±3.4°C (95% CI), with both the warmest and coldest data points falling within different stages of MIS M2. The average Δ_{47}-based BWT across the full study interval is 7.7±1.0°C (95% CI).

Our calculated record of $\delta^{18}O_{sw}$ (Fig. 3e) indicates an average of 1.1±0.3‰ (2σ) over the study interval, considerably higher than the present bottom water $\delta^{18}O_{sw}$ at Site U1308 of 0.25‰ (LeGrande and Schmidt, 2006). Similarly to Site 849, there is an apparent trend of decreasing values over the record — with somewhat higher $\delta^{18}O_{sw}$ before and during MIS M2 than afterwards. However, the significantly lower temporal resolution of the Site U1308 $\delta^{18}O_{sw}$ record makes this finding more uncertain than is the case for the Pacific.

12
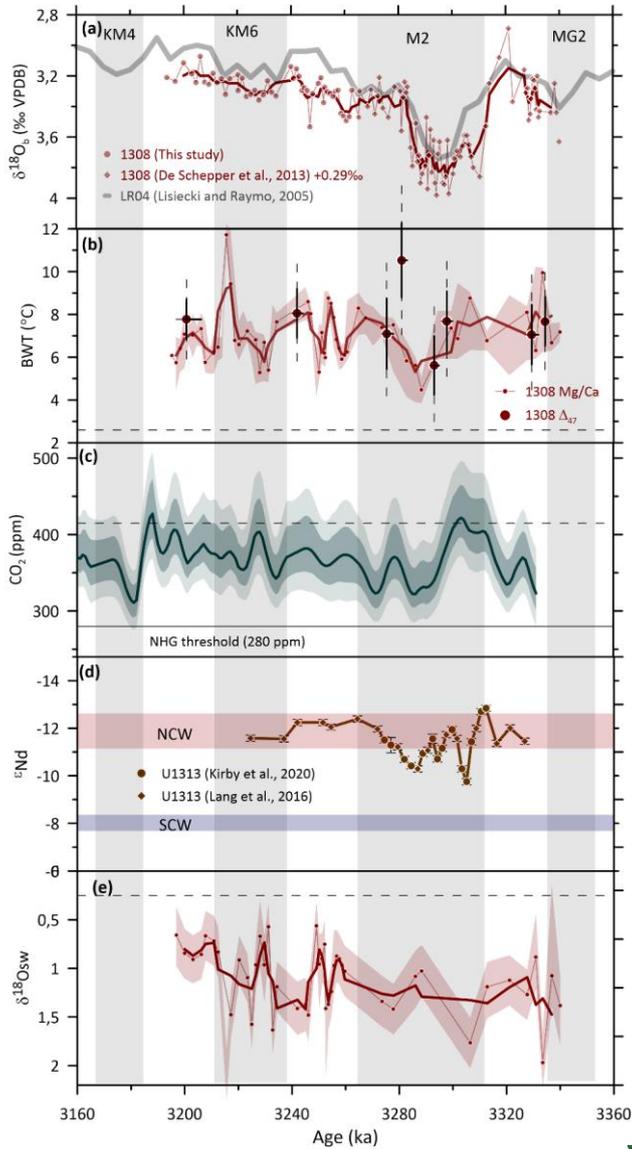
Figure 3. Climate indicators and results from North Atlantic IODP Site U1308. All horizontal stippled lines indicate modern values (CO_2 = 2022). (a) Benthic foraminiferal $\delta^{18}O$ from Site U1308 (shown with 3pt running mean and global benthic foraminiferal $\delta^{18}O$ stack. (b) U1308 temperature records Mg/Ca temperatures shown with 3pt running mean. Horizontal error bars on Δ_{47} temperatures indicate the age range of all individual samples used for each data point. Temperature uncertainties are expressed as solid (68% CI) and stippled (95% CI) bars. (c) Interpolated 1 ka resolution $\delta^{11}B$-derived CO_2 estimates from de la Vega et al. (2020). Confidence intervals expressed as dark (68%) and light (95%) shading. (d) fish debris Nd isotope data from North Atlantic IODP Site U1313 (Lang et al., 2016; Kirby et al., 2020). Estimates of SCW and NCW end-member ε_{Nd} composition following Lang et al., (2016). (e) calculated $\delta^{18}O_{sw}$ shown with a linear regression to highlight the overall trend (shading = 95% CI). Shaded envelopes on Mg/Ca temperatures and $\delta^{18}O_{sw}$ represent 2σ uncertainties modelled with PSU solver (Thirumalai et al., 2016).

Moved (insertion) [5]: . Confidence intervals expressed as dark (68%) and light (95%) shading. (d) fish debris Nd isotope data from North Atlantic IODP Site U1313 (Lang et al., 2016; Kirby et al., 2020). Estimates of SCW and NCW end-member ε_{Nd} composition following Lang et al., (2016). (e) calculated $\delta^{18}O_{sw}$ shown with a linear regression to highlight the overall trend (shading = 95% CI).

4 Discussion

4.1 Comparison between Mg/Ca and Δ_{47} temperatures

Comparison of our Mg/Ca- and Δ_{47}-based BWT records reveal good proxy agreement at both our Pacific and North Atlantic sites. At Pacific Site 849, all Δ_{47} temperatures are within error (95% CI) of the Mg/Ca-based record (Fig. 2b). The two proxies suggest similar average temperatures (Mg/Ca=~2.5±1.2°C, Δ_{47}=3.5±0.8°C), 1–2°C warmer than modern BWT at this site. At North Atlantic Site U1308, both proxies record similar average temperatures (Mg/Ca=7.2±1.5°C, Δ_{47}=7.7±1.0°C) approximately 4.5°C warmer than modern BWTs at this location (Fig. 3b). The Δ_{47}-based temperature at 3.280 Ma (10.5±3.4°C) is considerably warmer than three Mg/Ca-derived temperatures generated on some of the same samples (6.2–7.4°C). We find no obvious explanation for this discrepancy. None of the individual Δ_{47} replicates (n=32) are classified as outliers according to our criteria (4x SD), and the $\delta^{18}O_b$ values measured alongside the Δ_{47} are in excellent agreement with $\delta^{18}O_b$ measured separately (Fig. 4). It is possible that our Mg/Ca is underestimating BWT warming at the termination of M2, although we find this explanation to be unlikely. Extreme bottom-water warming at this time is not supported by either of the proxy records from the Pacific (Fig. 2b), or by the $\delta^{18}O_b$ records from either site (Fig. 2a and Fig. 3a). Furthermore, no available SST records from the high-latitude North Atlantic indicate such warming (e.g. Lawrence et al., 2009; Bachem et al., 2017; Clotten et al., 2018). We therefore conclude that this single Δ_{47}-based temperature likely overestimates BWTs at the termination of MIS M2. The otherwise good agreement between the proxies at both study sites adds confidence to our approach and supports the choice of the Mg/Ca calibration and other input parameters for Mg/Ca temperatures.

Deleted: °C±0.8

Deleted: °C

Deleted: °C

Deleted: °C

Deleted: °C

14
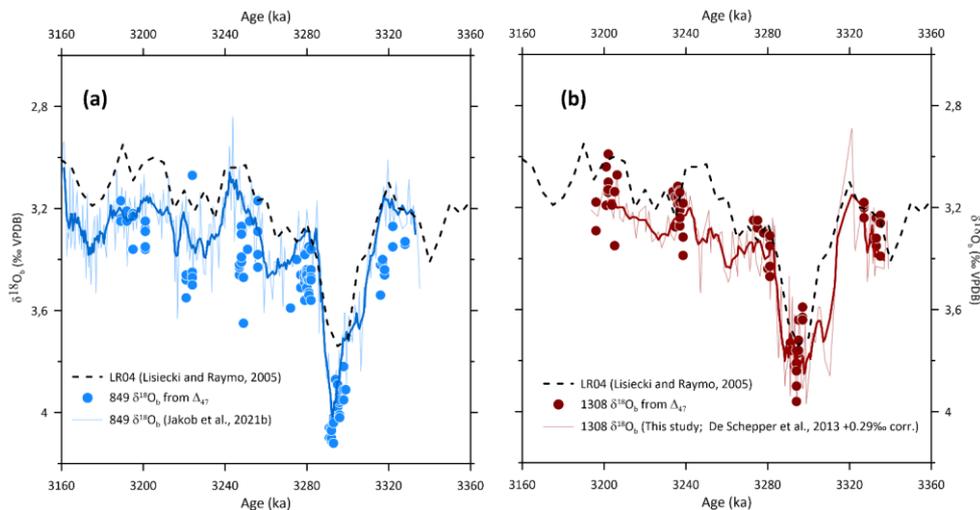
Figure 4. δ¹⁸O_b from individual Δ₄₇ measurements of Uvigerina spp. and Cibicidoides spp. (normalized to equilibrium following Shackleton et al., 1984)) from (a) Pacific ODP Site 849 and (b) North Atlantic Site U1308

490

4.2 Warm and salty deep North Atlantic

Previously published North Atlantic BWT reconstructions from the Pliocene have produced contradictory results. While ostracod-based Mg/Ca records from numerous sites in the deep North and South Atlantic suggest mid-Piacenzian temperatures were broadly similar to today, at around 2–3°C (Dwyer et al., 1995; Cronin et al., 2005; Dwyer and Chandler, 2009), studies based on Mg/Ca from benthic foraminifera indicate average temperatures of up to ~6°C — more than 3°C warmer than present (Bartoli et al., 2005; Sosdian and Rosenthal, 2009). Our paired benthic foraminiferal Mg/Ca and Δ₄₇ records suggest even warmer temperatures than previously estimated, with both proxies recording average BWTs above 7°C. We note that none of these previously published Mg/Ca-derived BWT records for the Pliocene were adjusted for estimated changes in Mg/Ca_sw. While the record of Sosdian and Rosenthal (2009) (3.150–0 Ma) does not overlap with our new Site U1308 record, recalculating (see Suppl. information and Fig. S6) their data produces average temperatures for their mid-Piacenzian interval closest to our records (3.150–3.0 Ma, ~7.7°C) that are in excellent agreement with our Mg/Ca and Δ₄₇ records. The records of Bartoli et al. (2005) cannot be recalculated in their published format.

Our new records indicate that BWTs in the deep North Atlantic Ocean were elevated by ~4.5–5.0°C relative to modern, considerably more than the estimated global average surface warming of 2–3°C relative to the pre-industrial during the MIS

15

| Deleted: mid- |
| Deleted: Pliocene |
| Deleted: change |
| Deleted: Pliocene |

510 KM5c time slice (McClymont et al., 2020; Haywood et al., 2020). Sea surface temperature reconstructions from the mPWP suggest that warming was particularly pronounced in the high northern latitudes, and possibly more so in the North Atlantic than at comparable latitudes in the Pacific (McClymont et al. 2020). Our records are in fact in good agreement with the PRISM (Pliocene Research, Interpretation and Synoptic Mapping) dataset, which reconstructs SSTs 4–5°C warmer than today in the source region of NADW (Dowsett et al., 2009a, b).

The deep water filling the North Atlantic was not just warmer, but likely also more saline than today. Our average calculated deep North Atlantic $\delta^{18}O_{sw}$ of 1.1‰ for the mid-Piacenzian is considerably higher than its present value of 0.25‰ and similar to values observed in surface water in the Mediterranean Sea and North Atlantic Subtropical gyre today. Given the paucity of
520 information about $\delta^{18}O_{sw}$-salinity relationships for the Pliocene, an exact quantification is difficult. However, we find it likely than this greatly elevated $\delta^{18}O_{sw}$ is reflective of a considerable increase in salinity compared to today. This would have aided the formation of warm Northern-sourced deep water by offsetting the buoyancy effect of the elevated temperature and may help explain how this water mass was sufficiently dense to fill the abyssal Atlantic despite potential competition from other, colder deep water masses sourced elsewhere. This salinification of the deep North Atlantic is supported by recent modelling
525 efforts. Weiffenbach et al. (2023) show that an increase in salinity in the high latitude North Atlantic is a consistent feature in the PlioMIP2 (Pliocene Model Intercomparison Project Phase 2) ensemble. In these models, a closed Bering Strait and Canadian Archipelago (Haywood et al., 2020) results in dramatically lower freshwater transport from the Arctic Ocean into the North Atlantic, which in turn contributes to elevated salinity (~2 PSU) in the Labrador Sea and the subpolar (40–60°C) North Atlantic. The PlioMIP2 ensemble also simulates lower precipitation-evaporation (P-E) over the Labrador Sea and
530 subtropical Atlantic (Feng et al., 2022), further contributing to elevated surface salinity in these regions.

4.3 Pacific–Atlantic temperature gradient

The deep Atlantic and Pacific Mg/Ca and Δ_{47} records confirm a large temperature gradient between these basins during the mid-Piacenzian (Fig. 5a). At the depth of our study sites (~3800 m), bottom water masses bathing the deep North Atlantic
535 today are slightly warmer (2.6°C vs. 1.6°C) and saltier (34.9 vs 34.7 PSU) than in the Pacific (Locarnini et al., 2013). The existence of a large temperature gradient of up to 4°C between these two basins in the Pliocene was first suggested by Woodard et al. (2014). Their foraminiferal Mg/Ca-based BWTs from ODP 1208 suggest temperatures in the North Pacific were possibly somewhat colder than today (when adjusted for Mg/Ca$_{sw}$ — see suppl. information and Fig. S6) during the mid-Piacenzian. In contrast, at Site 849 we observe warmer BWTs during the mid-Piacenzian compared to today. At face value, this discrepancy
540 would suggest that different water masses influenced the North Pacific and the central Pacific. As deep-water formation in the North Pacific has been suggested for the Pliocene (Burls et al., 2017; Shankle et al., 2021; Ford et al., 2022), it is possible that temperatures at Site 1208 were more directly influenced by this water mass and are thus more representative of the Pacific

16

Ocean as a whole than those at Site 849. It is however important to keep in mind that the absolute Mg/Ca-based temperatures are highly calibration dependent and are currently only cross-validated with Δ_{47} at our study sites.

Nevertheless, our new records substantiate the main interpretation of Woodard et al. (2014) that the deep North Atlantic Ocean was significantly warmer than the deep Pacific Ocean during the mid-Piacenzian (Fig 5a). We also document a large offset in $\delta^{18}O_{sw}$ between the deep Pacific (0.0‰) and deep North Atlantic Ocean (1.1‰, Fig 5b), likely reflecting a marked salinity gradient between the saltier Atlantic and fresher Pacific oceans. With respect to the ocean-wide salinity budget, a slight freshening of the deep Pacific is likely considering the strong salinification of the much narrower deep North Atlantic inferred from our records. We interpret our results to indicate that the deep Pacific and North Atlantic oceans were bathed by water masses with distinctly different physical properties during the mid-Pliocene. Hypothetically, one possible explanation for the observed temperature gradient, if water mass mixing was identical to today, could be that the Southern Ocean end member cooled enough to compensate for the warm Atlantic waters to produce a cold Pacific end result. Given the globally warm surface conditions of the mid-Pliocene, this scenario is, however, rather unlikely. Another possibility is that the deep central Pacific was bathed by a water mass sourced from the North Pacific rather than from the Southern Ocean. While formation of NPDW has been suggested for the Pliocene (Burls et al., 2017; Shankle et al., 2021; Ford et al., 2022), the modelled spatial extent of NPDW during the mPWP does not support a large influence of this water mass on the abyssal central Pacific (Ford et al., 2022). Instead, we consider it more likely that limited oceanic exchange occurred between the two basins at this time. This suggests a fundamentally different mode of ocean circulation or mixing compared to the present, where heat and salt is distributed from the North Atlantic into the Pacific. Although some surface exchange between the Pacific and Atlantic Oceans through the Central American Seaway (CAS) may have still occurred in the mid-Piacenzian, the seaway was too shallow as this point to significantly influence deep ocean circulation (e.g. Straume et al., 2020).

Due to the lack of comparable BWT records from the Pacific and Atlantic before 3.3 Ma, it is unclear when the mid-Piacenzian circulation state commenced. Determining this would likely provide further clues of the effects it had on the warm climates of the Pliocene. Woodard et al. (2014) suggest that this mode of circulation was abruptly terminated at 2.7 Ma, when the temperature gradient between the North Atlantic and North Pacific was reduced from ~4C° to ~1C°. They therefore suggest this as a potential contributing factor for iNHG. However, it is unclear if the large gradient between the central Pacific and North Atlantic also ceased at 2.7 Ma. Furthermore, as the North Pacific BWT record ends at 2.5 Ma, it remains unclear if the gradient between this site and the North Atlantic was permanently reduced after iNHG or reemerged at points during the Pleistocene.

17

4.4 Marine Isotope stage M2

Interrupting the warm and mostly stable, high CO_2 climate of the mid-Piacenzian is Marine Isotope Stage M2 (3.312–3.264 Ma), representing the largest positive benthic oxygen isotope excursion in the Pliocene prior to iNHG (Lisiecki and Raymo, 2005). The ~0.64‰ increase in the global $\delta^{18}O_b$ stack suggests either a major increase in land ice-volume, strong cooling of the deep ocean, or some combination thereof. Estimates of sea-level fall associated with this event range from relatively minor (Naish and Wilson, 2009; Rohling et al., 2014) to more than 60 meters below modern (Dwyer and Chandler, 2009), consistent with a very large build-up of ice on land. While the most conservative of these estimates could be explained by an expansion of the Antarctic ice sheet at that time — as is documented in Southern Ocean IRD records (e.g. Passchier, 2011; McKay et al., 2012) — the largest estimate would also require substantial glaciation of the Northern Hemisphere. Although sedimentological evidence suggests at least some ice-growth in the circum-Arctic during M2 (i.e. De Schepper et al., 2014 and references therein), there is no conclusive evidence for the existence of large Northern Hemisphere ice sheets at that time. Deconvolving the ice-volume signal from the benthic $\delta^{18}O$ record, which would help constrain the extent of glacial expansion and plausible scenarios for ice-sheet growth, has thus far been hampered by a lack of high-resolution BWT reconstructions from this time interval.

Our Pacific Mg/Ca record represents the highest-resolution BWT record for MIS M2 to date and it is the first record of sufficient temporal resolution to investigate potential leads and lags in the climate system. Our data suggest abrupt MIS M2 cooling of 3–4°C in the deep Central Pacific starting at ~3.30 Ma. This cooling appears to lag changes in benthic $\delta^{18}O$ (Jakob et al., 2021b, Fig. 2a, measured on the same samples) by approximately 20 kyr, but it is in phase with a decrease in CO_2 of approximately 100 ppm (de la Vega et al., 2020, Fig.2c, Fig. S7). We speculate that the early increase in $\delta^{18}O_b$ prior to the onset of M2, which is lacking a synchronous drop in BWT, represents an increase in global ice volume, and that the subsequent $\delta^{18}O_b$ increase reflects cooling of the deep ocean. Interpreting calculated bottom water $\delta^{18}O_{sw}$ entirely as a measure of ice volume suggests elevated ice volume (relative to present) during the entire early half of our 849 record (3.334–3.264), i.e., not only during the MIS M2 cooling event, but also during the preceding interglacial (MIS MG1) (Fig. 2e). Following the termination of MIS M2, a gradual change in $\delta^{18}O_{sw}$ implies a decrease in ice-volume relative to present. However, the large

19

830 spatial differences between North Atlantic and Pacific bottom water $\delta^{18}O_{sw}$ inferred from our records (Fig. 5b) complicates the interpretation of $\delta^{18}O_{sw}$ as entirely reflective of ice-volume — unless the variations are seen globally.

Our North Atlantic Site U1308 Mg/Ca record is of significantly lower temporal resolution than at Site 849. However, we observe MIS M2 BWT cooling of a similar amplitude as seen in the Central Pacific. While a lag in cooling relative to $\delta^{18}O_b$

835 also appears to exist in the North Atlantic (Fig. 3b), this finding is not as robust as in the Pacific. Despite the cooling observed during MIS M2, North Atlantic BWTs remain warmer than present throughout the event. This is in line with SST reconstructions from the North Atlantic and Nordic Seas showing that temperatures remained as warm or warmer than the Holocene average during MIS M2 (Lawrence et al., 2009; Bachem et al., 2017; De Schepper et al., 2013; Naafs et al., 2010). The sustained high-latitude warmth in the source region of NCW throughout MIS M2 inferred from our records add further

840 evidence that ice-sheet advance in the Northern Hemisphere was possibly limited to the circum-Arctic.

Based on benthic $\delta^{13}C$ and Nd-isotope records, Kirby et al. (2020) conclude that — unlike during early and late Pleistocene glacials such as MIS 100 and 2 — NCW largely prevailed in the deep North Atlantic Ocean during M2. This interpretation is supported by our BWT records showing that the large temperature gradient between the Pacific and North Atlantic was

845 maintained over M2 (Fig. 4a). Furthermore, fish debris Nd-isotope ratios from North Atlantic Site U1313 (Kirby et al., 2020, Fig. 3d) suggest that the smaller incursions of Southern Component Waters (SCW) peaked well before $\delta^{18}O_b$ and minima in BWT and atmospheric CO_2, further supporting that an influx of southern waters is not responsible for the observed cooling at Site U1308. This suggests global-scale cooling during MIS M2, with the source regions for both Southern- and Northern-sourced deep waters cooling concurrently.

850

Given the lack of major SCW incursions into the deep North Atlantic, and that cooling in the Pacific appears to be in-phase with CO_2 (de la Vega et al., 2020, Fig. 2c), we interpret our data to indicate that the deep Pacific, and not the Atlantic, was the ultimate sink for CO_2 sequestered from the atmosphere over this event, as was speculated by Kirby et al. (2020). We furthermore suggest the decrease in atmospheric CO_2 concentrations as the main driver behind the observed MIS M2 deep sea

855 cooling.

At Site 849, our Mg/Ca record reveals additional large changes in deep Pacific temperatures during the mPWP that have not previously been fully documented. Cooling events of similar amplitude to that of MIS M2 also occur during MIS KM4 and KM6, but these stages are not reflected as significant glacial events in the $\delta^{18}O_b$ record. This suggests that increases in $\delta^{18}O_{sw}$

860 compensated for the decreases in temperature, leaving $\delta^{18}O_b$ largely unaffected. Cooling during KM4 is associated with a CO_2 decrease of similar magnitude to that documented for MIS M2 (~100 ppm). Thus, despite the anomalous $\delta^{18}O_b$ excursion associated with MIS M2, this event does not appear to not be unique in terms of BWT cooling and atmospheric CO_2 decrease

Deleted: (de la Vega et al., 2020, Fig. 2c)

Deleted: M2

Deleted: mid-Pliocene

in the mid-Piacenzian. The amplitude of cooling observed at both sites during MIS M2 suggests that changes in benthic $\delta^{18}O$ associated with this cold stage were mostly driven by temperature change in the deep ocean rather than ice volume.

5. Conclusions

870 We present new benthic foraminiferal Mg/Ca and Δ_{47} records from Equatorial East Pacific Site 849 and North Atlantic Site U1308, spanning MIS M2 and the first half of the mid-Piacenzian Warm Period. We demonstrate that a large bottom water temperature gradient of >4°C existed between the deep Pacific and Atlantic basins at this time, in line with previous findings, and that the mid-Piacenzian deep ocean was less homogenous than at present not just in temperature, but also in $\delta^{18}O_{sw}$ and thus likely salinity. We propose that this was caused by limited oceanic exchange between the deep Atlantic and Pacific oceans, suggesting a fundamentally different mode of ocean circulation and/or mixing than at present. We furthermore find that both

875 basins cooled by 3–4°C during MIS M2, suggesting that the large positive oxygen isotope excursion associated with this event largely reflects global-scale cooling in the deep ocean—likely driven by decreasing CO_2 concentrations — rather than a substantial increase in ice volume on land. Our observation that cooling events of a similar amplitude also occurred in the following two "glacial" Marine Isotope Stages (KM4 and KM6) suggests that that the climatic impact of the M2 event was not as unique as suggested by the benthic $\delta^{18}O$ record alone, and that deep ocean temperatures in the mid-Piacenzian were

880 more variable than has previously been documented.

Data availability

The data from this paper are archived in the supplement (Table S1-6). In addition, all trace metal data, calculated Mg/Ca and Δ_{47} temperatures, and new stable isotope data are available at PANGAEA (https://**doi.org**/10.1594/PANGAEA.960832)

Author contribution

885 AHB, SLH, KAJ, OF and ANM initiated and designed the study. AHB generated and analyzed clumped isotope data under the supervision of EVG and ANM. SLH generated and analyzed clumped isotope data under the supervision of ANM. KAJ generated and analyzed Mg/Ca data under the supervision of OF. All the authors contributed to the palaeoceanographic interpretation. AHB wrote the paper with contributions from all co-authors.

Competing interests

890 The authors declare that they have no conflict of interest.

References

Arhan, M., Mercier, H., and Park, Y.-H.: On the deep water circulation of the eastern South Atlantic Ocean, Deep Sea Res. Part Oceanogr. Res. Pap., 50, 889–916, https://doi.org/10.1016/S0967-0637(03)00072-4, 2003.

Bachem, P. E., Risebrobakken, B., De Schepper, S., and McClymont, E. L.: Highly variable Pliocene sea surface conditions in the Norwegian Sea, Clim. Past, 13, 1153–1168, https://doi.org/10.5194/cp-13-1153-2017, 2017.

Barker, S., Greaves, M., and Elderfield, H.: A study of cleaning procedures used for foraminiferal Mg/Ca paleothermometry, Geochem. Geophys. Geosystems, 4, https://doi.org/10.1029/2003GC000559, 2003.

Bartoli, G., Sarnthein, M., Weinelt, M., Erlenkeuser, H., Garbe-Schönberg, D., and Lea, D. W.: Final closure of Panama and the onset of northern hemisphere glaciation, Earth Planet. Sci. Lett., 237, 33–44, https://doi.org/10.1016/j.epsl.2005.06.020, 2005.

Bernasconi, S. M., Daëron, M., Bergmann, K. D., Bonifacie, M., Meckler, A. N., Affek, H. P., Anderson, N., Bajnai, D., Barkan, E., Beverly, E., Blamart, D., Burgener, L., Calmels, D., Chaduteau, C., Clog, M., Davidheiser-Kroll, B., Davies, A., Dux, F., Eiler, J., Elliott, B., Fetrow, A. C., Fiebig, J., Goldberg, S., Hermoso, M., Huntington, K. W., Hyland, E., Ingalls, M., Jaggi, M., John, C. M., Jost, A. B., Katz, S., Kelson, J., Kluge, T., Kocken, I. J., Laskar, A., Leutert, T. J., Liang, D., Lucarelli, J., Mackey, T. J., Mangenot, X., Meinicke, N., Modestou, S. E., Müller, I. A., Murray, S., Neary, A., Packard, N., Passey, B. H., Pelletier, E., Petersen, S., Piasecki, A., Schauer, A., Snell, K. E., Swart, P. K., Tripati, A., Upadhyay, D., Vennemann, T., Winkelstern, I., Yarian, D., Yoshida, N., Zhang, N., and Ziegler, M.: InterCarb: A Community Effort to Improve Interlaboratory Standardization of the Carbonate Clumped Isotope Thermometer Using Carbonate Standards, Geochem. Geophys. Geosystems, 22, e2020GC009588, https://doi.org/10.1029/2020GC009588, 2021.

22

Burke, K. D., Williams, J. W., Chandler, M. A., Haywood, A. M., Lunt, D. J., and Otto-Bliesner, B. L.: Pliocene and Eocene provide best analogs for near-future climates, Proc. Natl. Acad. Sci., 115, 13288–13293, https://doi.org/10.1073/pnas.1809600115, 2018.

935 Burls, N. J., Fedorov, A. V., Sigman, D. M., Jaccard, S. L., Tiedemann, R., and Haug, G. H.: Active Pacific meridional overturning circulation (PMOC) during the warm Pliocene, Sci. Adv., 3, e1700156, https://doi.org/10.1126/sciadv.1700156, 2017.

Clotten, C., Stein, R., Fahl, K., and De Schepper, S.: Seasonal sea ice cover during the warm Pliocene: Evidence from the Iceland Sea (ODP Site 907), Earth Planet. Sci. Lett., 481, 61–72, https://doi.org/10.1016/j.epsl.2017.10.011, 2018.

940 Coggon, R. M., Teagle, D. A. H., Smith-Duque, C. E., Alt, J. C., and Cooper, M. J.: Reconstructing Past Seawater Mg/Ca and Sr/Ca from Mid-Ocean Ridge Flank Calcium Carbonate Veins, Science, 327, 1114–1117, https://doi.org/10.1126/science.1182252, 2010.

Cronin, T. M., Dowsett, H. J., Dwyer, G. S., Baker, P. A., and Chandler, M. A.: Mid-Pliocene deep-sea bottom-water temperatures based on ostracode Mg/Ca ratios, Mar. Micropaleontol., 54, 249–261,
945 https://doi.org/10.1016/j.marmicro.2004.12.003, 2005.

De Schepper, S., Groeneveld, J., Naafs, B. D. A., Van Renterghem, C., Hennissen, J., Head, M., Louwye, S., and Fabian, K.: Northern hemisphere glaciation during the globally warm early Late Pliocene, PLOS ONE, 8, http://dx.doi.org/10.1371/journal.pone.0081508, 2013.

De Schepper, S., Gibbard, P. L., Salzmann, U., and Ehlers, J.: A global synthesis of the marine and terrestrial evidence for
950 glaciation during the Pliocene Epoch, Earth-Sci. Rev., 135, 83–102, https://doi.org/10.1016/j.earscirev.2014.04.003, 2014.

Dickson, J. A. D.: Echinoderm Skeletal Preservation: Calcite-Aragonite Seas and the Mg/Ca Ratio of Phanerozoic Oceans, J. Sediment. Res., 74, 355–365, https://doi.org/10.1306/112203740355, 2004.

Dowsett, H. J., Robinson, M. M., and Foley, K. M.: Pliocene three-dimensional global ocean temperature reconstruction, Clim. Past, 5, 769–783, https://doi.org/10.5194/cp-5-769-2009, 2009a.

955 Dowsett, H. J., Chandler, M. A., and Robinson, M. M.: Surface temperatures of the Mid-Pliocene North Atlantic Ocean: implications for future climate, Philos. Trans. R. Soc. Math. Phys. Eng. Sci., 367, 69–84, https://doi.org/10.1098/rsta.2008.0213, 2009b.

Dowsett, H. J., Robinson, M. M., Haywood, A. M., Hill, D. J., Dolan, A. M., Stoll, D. K., Chan, W.-L., Abe-Ouchi, A., Chandler, M. A., Rosenbloom, N. A., Otto-Bliesner, B. L., Bragg, F. J., Lunt, D. J., Foley, K. M., and Riesselman, C. R.:
960 Assessing confidence in Pliocene sea surface temperatures to evaluate predictive models, Nat. Clim. Change, 2, 365–371, https://doi.org/10.1038/nclimate1455, 2012.

Dumitru, O. A., Austermann, J., Polyak, V. J., Fornós, J. J., Asmerom, Y., Ginés, J., Ginés, A., and Onac, B. P.: Constraints on global mean sea level during Pliocene warmth, Nature, 574, 233–236, https://doi.org/10.1038/s41586-019-1543-2, 2019.

Dwyer, G. S. and Chandler, M. A.: Mid-Pliocene sea level and continental ice volume based on coupled benthic Mg/Ca
965 palaeotemperatures and oxygen isotopes, Philos. Trans. R. Soc. Math. Phys. Eng. Sci., 367, 157–168, https://doi.org/10.1098/rsta.2008.0222, 2009.

23

Dwyer, G. S., Cronin, T. M., Baker, P. A., Raymo, M. E., Buzas, J. S., and Corrège, T.: North Atlantic Deepwater Temperature Change During Late Pliocene and Late Quaternary Climatic Cycles, Science, 270, 1347–1351, https://doi.org/10.1126/science.270.5240.1347, 1995.

970 Eiler, J. M.: Paleoclimate reconstruction using carbonate clumped isotope thermometry, Quat. Sci. Rev., 30, 3575–3588, https://doi.org/10.1016/j.quascirev.2011.09.001, 2011.

Elderfield, H., Yu, J., Anand, P., Kiefer, T., and Nyland, B.: Calibrations for benthic foraminiferal Mg/Ca paleothermometry and the carbonate ion hypothesis, Earth Planet. Sci. Lett., 250, 633–649, https://doi.org/10.1016/j.epsl.2006.07.041, 2006.

Evans, D., Brierley, C., Raymo, M. E., Erez, J., and Müller, W.: Planktic foraminifera shell chemistry response to seawater
975 chemistry: Pliocene–Pleistocene seawater Mg/Ca, temperature and sea level change, Earth Planet. Sci. Lett., 438, 139–148, https://doi.org/10.1016/j.epsl.2016.01.013, 2016.

Expedition 303 Scientists: Site U1308, in: North Atlantic Climate, vol. 303/306, Procedings of the Integrated Ocean Drilling Program, 2006.

Fedorov, A. V., Dekens, P. S., McCarthy, M., Ravelo, A. C., deMenocal, P. B., Barreiro, M., Pacanowski, R. C., and Philander,
980 S. G.: The Pliocene Paradox (Mechanisms for a Permanent El Niño), Science, 312, 1485–1489, https://doi.org/10.1126/science.1122666, 2006.

Feng, R., Bhattacharya, T., Otto-Bliesner, B. L., Brady, E. C., Haywood, A. M., Tindall, J. C., Hunter, S. J., Abe-Ouchi, A., Chan, W.-L., Kageyama, M., Contoux, C., Guo, C., Li, X., Lohmann, G., Stepanek, C., Tan, N., Zhang, Q., Zhang, Z., Han, Z., Williams, C. J. R., Lunt, D. J., Dowsett, H. J., Chandan, D., and Peltier, W. R.: Past terrestrial hydroclimate sensitivity
985 controlled by Earth system feedbacks, Nat. Commun., 13, 1306, https://doi.org/10.1038/s41467-022-28814-7, 2022.

Ford, H. L., Sosdian, S. M., Rosenthal, Y., and Raymo, M. E.: Gradual and abrupt changes during the Mid-Pleistocene Transition, Quat. Sci. Rev., 148, 222–233, https://doi.org/10.1016/j.quascirev.2016.07.005, 2016.

Ford, H. L., Burls, N. J., Jacobs, P., Jahn, A., Caballero-Gill, R. P., Hodell, D. A., and Fedorov, A. V.: Sustained mid-Pliocene warmth led to deep water formation in the North Pacific, Nat. Geosci., 15, 658–663, https://doi.org/10.1038/s41561-022-
990 00978-3, 2022.

Ghosh, P., Adkins, J., Affek, H., Balta, B., Guo, W., Schauble, E. A., Schrag, D., and Eiler, J. M.: 13C–18O bonds in carbonate minerals: A new kind of paleothermometer, Geochim. Cosmochim. Acta, 70, 1439–1456, https://doi.org/10.1016/j.gca.2005.11.014, 2006.

Grant, G. R., Naish, T. R., Dunbar, G. B., Stocchi, P., Kominz, M. A., Kamp, P. J. J., Tapia, C. A., McKay, R. M., Levy, R.
995 H., and Patterson, M. O.: The amplitude and origin of sea-level variability during the Pliocene epoch, Nature, 574, 237–241, https://doi.org/10.1038/s41586-019-1619-z, 2019.

Greaves, M., Caillon, N., Rebaubier, H., Bartoli, G., Bohaty, S., Cacho, I., Clarke, L., Cooper, M., Daunt, C., Delaney, M., deMenocal, P., Dutton, A., Eggins, S., Elderfield, H., Garbe-Schoenberg, D., Goddard, E., Green, D., Groeneveld, J., Hastings, D., Hathorne, E., Kimoto, K., Klinkhammer, G., Labeyrie, L., Lea, D. W., Marchitto, T., Martínez-Botí, M. A., Mortyn, P. G.,
1000 Ni, Y., Nuernberg, D., Paradis, G., Pena, L., Quinn, T., Rosenthal, Y., Russell, A., Sagawa, T., Sosdian, S., Stott, L., Tachikawa, K., Tappa, E., Thunell, R., and Wilson, P. A.: Interlaboratory comparison study of calibration standards for foraminiferal Mg/Ca thermometry, Geochem. Geophys. Geosystems, 9, https://doi.org/10.1029/2008GC001974, 2008.

Haug, G. H. and Tiedemann, R.: Effect of the formation of the Isthmus of Panama on Atlantic Ocean thermohaline circulation, Nature, 393, 673–676, https://doi.org/10.1038/31447, 1998.

24

Haywood, A. M., Dolan, A. M., Pickering, S. J., Dowsett, H. J., McClymont, E. L., Prescott, C. L., Salzmann, U., Hill, D. J., Hunter, S. J., Lunt, D. J., Pope, J. O., and Valdes, P. J.: On the identification of a Pliocene time slice for data–model comparison, Philos. Trans. R. Soc. Math. Phys. Eng. Sci., 371, 20120515, https://doi.org/10.1098/rsta.2012.0515, 2013.

Haywood, A. M., Tindall, J. C., Dowsett, H. J., Dolan, A. M., Foley, K. M., Hunter, S. J., Hill, D. J., Chan, W.-L., Abe-Ouchi, A., Stepanek, C., Lohmann, G., Chandan, D., Peltier, W. R., Tan, N., Contoux, C., Ramstein, G., Li, X., Zhang, Z., Guo, C., Nisancioglu, K. H., Zhang, Q., Li, Q., Kamae, Y., Chandler, M. A., Sohl, L. E., Otto-Bliesner, B. L., Feng, R., Brady, E. C., von der Heydt, A. S., Baatsen, M. L. J., and Lunt, D. J.: The Pliocene Model Intercomparison Project Phase 2: large-scale climate features and climate sensitivity, Clim. Past, 16, 2095–2123, https://doi.org/10.5194/cp-16-2095-2020, 2020.

Hodell, D. A., Channell, J. E. T., Curtis, J. H., Romero, O. E., and Röhl, U.: Onset of "Hudson Strait" Heinrich events in the eastern North Atlantic at the end of the middle Pleistocene transition (~640 ka)?, Paleoceanography, 23, https://doi.org/10.1029/2008PA001591, 2008.

Hu, B., Radke, J., Schlüter, H.-J., Heine, F. T., Zhou, L., and Bernasconi, S. M.: A modified procedure for gas-source isotope ratio mass spectrometry: the long-integration dual-inlet (LIDI) methodology and implications for clumped isotope measurements, Rapid Commun. Mass Spectrom., 28, 1413–1425, https://doi.org/10.1002/rcm.6909, 2014.

Jakob, K. A., Wilson, P. A., Pross, J., Ezard, T. H. G., Fiebig, J., Repschläger, J., and Friedrich, O.: A new sea-level record for the Neogene/Quaternary boundary reveals transition to a more stable East Antarctic Ice Sheet, Proc. Natl. Acad. Sci., 117, 30980–30987, https://doi.org/10.1073/pnas.2004209117, 2020.

Jakob, K. A., Pross, J., Link, J. M., Blaser, P., Braaten, A. H., and Friedrich, O.: Deep-ocean circulation in the North Atlantic during the Plio-Pleistocene intensification of Northern Hemisphere Glaciation (~2.65–2.4 Ma), Mar. Micropaleontol., 165, 101998, https://doi.org/10.1016/j.marmicro.2021.101998, 2021a.

Jakob, K. A., Ho, S. L., Meckler, A. N., Pross, J., Fiebig, J., Keppler, F., and Friedrich, O.: Stable Biological Production in the Eastern Equatorial Pacific Across the Plio-Pleistocene Transition (~3.35–2.0 Ma), Paleoceanogr. Paleoclimatology, 36, e2020PA003965, https://doi.org/10.1029/2020PA003965, 2021b.

John, C. M. and Bowen, D.: Community software for challenging isotope analysis: First applications of 'Easotope' to clumped isotopes, Rapid Commun. Mass Spectrom., 30, 2285–2300, https://doi.org/10.1002/rcm.7720, 2016.

Kirby, N., Bailey, I., Lang, D. C., Brombacher, A., Chalk, T. B., Parker, R. L., Crocker, A. J., Taylor, V. E., Milton, J. A., Foster, G. L., Raymo, M. E., Kroon, D., Bell, D. B., and Wilson, P. A.: On climate and abyssal circulation in the Atlantic Ocean during late Pliocene marine isotope stage M2, ~3.3 million years ago, Quat. Sci. Rev., 250, 106644, https://doi.org/10.1016/j.quascirev.2020.106644, 2020.

Kotov, S. and Pälike, H.: QAnalySeries: a cross-platform time series tuning and analysis tool, Earth Space Sci. Open Arch., 1, https://doi.org/10.1002/essoar.10500226.1, 2018.

Kwiek, P. B. and Ravelo, A. C.: Pacific Ocean intermediate and deep water circulation during the Pliocene, Palaeogeogr. Palaeoclimatol. Palaeoecol., 154, 191–217, https://doi.org/10.1016/S0031-0182(99)00111-X, 1999.

Lang, D. C., Bailey, I., Wilson, P. A., Chalk, T. B., Foster, G. L., and Gutjahr, M.: Incursions of southern-sourced water into the deep North Atlantic during late Pliocene glacial intensification, Nat. Geosci., 9, 375–379, https://doi.org/10.1038/ngeo2688, 2016.

Laskar, J., Robutel, P., Joutel, F., Gastineau, M., Correia, A. C. M., and Levrard, B.: A long-term numerical solution for the insolation quantities of the Earth, Astron. Astrophys., 428, 261–285, https://doi.org/10.1051/0004-6361:20041335, 2004.

Lawrence, K. T., Herbert, T. D., Brown, C. M., Raymo, M. E., and Haywood, A. M.: High-amplitude variations in North Atlantic sea surface temperature during the early Pliocene warm period: VARIABLE PLIOCENE NORTH ATLANTIC SSTS, Paleoceanography, 24, n/a-n/a, https://doi.org/10.1029/2008PA001669, 2009.

Lear, C. H., Elderfield, H., and Wilson, P. A.: Cenozoic Deep-Sea Temperatures and Global Ice Volumes from Mg/Ca in Benthic Foraminiferal Calcite, Science, 287, 269–272, https://doi.org/10.1126/science.287.5451.269, 2000.

Lear, C. H., Rosenthal, Y., and Slowey, N.: Benthic foraminiferal Mg/Ca-paleothermometry: a revised core-top calibration, Geochim. Cosmochim. Acta, 66, 3375–3387, https://doi.org/10.1016/S0016-7037(02)00941-9, 2002.

Lear, C. H., Mawbey, E. M., and Rosenthal, Y.: Cenozoic benthic foraminiferal Mg/Ca and Li/Ca records: Toward unlocking temperatures and saturation states, Paleoceanography, 25, https://doi.org/10.1029/2009PA001880, 2010.

Lear, C. H., Coxall, H. K., Foster, G. L., Lunt, D. J., Mawbey, E. M., Rosenthal, Y., Sosdian, S. M., Thomas, E., and Wilson, P. A.: Neogene ice volume and ocean temperatures: Insights from infaunal foraminiferal Mg/Ca paleothermometry, Paleoceanography, 30, 1437–1454, https://doi.org/10.1002/2015PA002833, 2015.

LeGrande, A. N. and Schmidt, G. A.: Global gridded data set of the oxygen isotopic composition in seawater, Geophys. Res. Lett., 33, https://doi.org/10.1029/2006GL026011, 2006.

Lisiecki, L. E. and Raymo, M. E.: A Pliocene-Pleistocene stack of 57 globally distributed benthic δ18O records, Paleoceanography, 20, https://doi.org/10.1029/2004PA001071, 2005.

Locarnini, R. A., Mishonov, A. V., Antonov, J. I., Boyer, T. P., Garcia, H. E., Baranova, O. K., Zweng, M. M., Paver, C. R., Reagan, J. R., Johnson, D. R., Hamilton, M., and Seidov, D.: World Ocean Atlas 2013, in: World Ocean Atlas, vol. Volume 1: Temperature, NOAA Atlas NESDIS, 40 pp., 2013.

Marchitto, T. M., Curry, W. B., Lynch-Stieglitz, J., Bryan, S. P., Cobb, K. M., and Lund, D. C.: Improved oxygen isotope temperature calibrations for cosmopolitan benthic foraminifera, Geochim. Cosmochim. Acta, 130, 1–11, https://doi.org/10.1016/j.gca.2013.12.034, 2014.

Martínez-Botí, M. A., Foster, G. L., Chalk, T. B., Rohling, E. J., Sexton, P. F., Lunt, D. J., Pancost, R. D., Badger, M. P. S., and Schmidt, D. N.: Plio-Pleistocene climate sensitivity evaluated using high-resolution CO2 records, Nature, 518, 49-54K, http://dx.doi.org/10.1038/nature14145, 2015.

Mayer, L. A., Pisias, N. G., Janecek, T. R., Baldauf, J. G., Bloomer, S. F., Dadey, K. A., Emeis, K.-C., Farrell, J., Flores, J. A., Galimov, E. M., Hagelberg, T. K., Holler, P., Hovan, S. A., Iwai, M., and Kem, A. E. S.: Proceedings of the Ocean Drilling Program. VOLUME 13 8 INITIAL REPORTS PARTI EASTERN EQUATORIAL PACIFIC Covering Leg 138 of the cruises of the Drilling Vessel JOIDES Resolution, Balboa, Panama, to San Diego, California, Sites 844-854, 6 May 1991-5 July 19, 28, 1992.

McClymont, E. L., Ford, H. L., Ho, S. L., Tindall, J. C., Haywood, A. M., Alonso-Garcia, M., Bailey, I., Berke, M. A., Littler, K., Patterson, M. O., Petrick, B., Peterse, F., Ravelo, A. C., Risebrobakken, B., De Schepper, S., Swann, G. E. A., Thirumalai, K., Tierney, J. E., van der Weijst, C., White, S., Abe-Ouchi, A., Baatsen, M. L. J., Brady, E. C., Wing-Le, C., Chandan, D., Feng, R., Guo, C., von der Heydt, A. S., Hunter, S., Li, X., Lohmann, G., Nisancioglu, K. H., Otto-Bliesner, B. L., Peltier, W. R., Stepanek, C., and Zhang, Z.: Lessons from a high-CO2 world: an ocean view from ~3 million years ago, Clim. Past, 16, 1599–1615, http://dx.doi.org.pva.uib.no/10.5194/cp-16-1599-2020, 2020.

Deleted: Lynch-Stieglitz, J., Curry, W. B., and Slowey, N.: A geostrophic transport estimate for the Florida Current from the oxygen isotope composition of benthic foraminifera, Paleoceanography, 14, 360–373, https://doi.org/10.1029/1999PA900001, 1999.¶

McKay, R., Naish, T., Carter, L., Riesselman, C., Dunbar, R., Sjunneskog, C., Winter, D., Sangiorgi, F., Warren, C., Pagani, M., Schouten, S., Willmott, V., Levy, R., DeConto, R., and Powell, R. D.: Antarctic and Southern Ocean influences on Late Pliocene global cooling, Proc. Natl. Acad. Sci., 109, 6423–6428, https://doi.org/10.1073/pnas.1112248109, 2012.

Meckler, A. N., Ziegler, M., Millán, M. I., Breitenbach, S. F. M., and Bernasconi, S. M.: Long-term performance of the Kiel carbonate device with a new correction scheme for clumped isotope measurements, Rapid Commun. Mass Spectrom., 28, 1705–1715, https://doi.org/10.1002/rcm.6949, 2014.

Meinicke, N., Ho, S. L., Hannisdal, B., Nürnberg, D., Tripati, A., Schiebel, R., and Meckler, A. N.: A robust calibration of the clumped isotopes to temperature relationship for foraminifers, Geochim. Cosmochim. Acta, 270, 160–183, https://doi.org/10.1016/j.gca.2019.11.022, 2020.

Meinicke, N., Reimi, M. A., Ravelo, A. C., and Meckler, A. N.: Coupled Mg/Ca and Clumped Isotope Measurements Indicate Lack of Substantial Mixed Layer Cooling in the Western Pacific Warm Pool During the Last ~5 Million Years, Paleoceanogr. Paleoclimatology, 36, e2020PA004115, https://doi.org/10.1029/2020PA004115, 2021.

Miller, K. G., Wright, J. D., Browning, J. V., Kulpecz, A., Kominz, M., Naish, T. R., Cramer, B. S., Rosenthal, Y., Peltier, W. R., and Sosdian, S.: High tide of the warm Pliocene: Implications of global sea level for Antarctic deglaciation, Geology, 40, 407–410, https://doi.org/10.1130/G32869.1, 2012.

Mix, A. C., Pisias, N. G., Rugh, W., Wilson, J., Morey, A., and Hagelberg, T. K.: Benthic foraminifer stable isotope record from Site 849 (0-5 Ma): local and global climate changes, Proc. Ocean Drill. Program Sci. Results, 138, 371–412, https://doi.org/10.2973/odp.proc.sr.138.1995, 1995.

Naafs, B. D. A., Stein, R., Hefter, J., Khélifi, N., De Schepper, S., and Haug, G. H.: Late Pliocene changes in the North Atlantic Current, Earth Planet. Sci. Lett., 298, 434–442, https://doi.org/10.1016/j.epsl.2010.08.023, 2010.

Naish, T. R. and Wilson, G. S.: Constraints on the amplitude of Mid-Pliocene (3.6–2.4 Ma) eustatic sea-level fluctuations from the New Zealand shallow-marine sediment record, Philos. Trans. R. Soc. Math. Phys. Eng. Sci., 367, 169–187, https://doi.org/10.1098/rsta.2008.0223, 2009.

de Nooijer, W., Zhang, Q., Li, Q., Zhang, Q., Li, X., Zhang, Z., Guo, C., Nisancioglu, K. H., Haywood, A. M., Tindall, J. C., Hunter, S. J., Dowsett, H. J., Stepanek, C., Lohmann, G., Otto-Bliesner, B. L., Feng, R., Sohl, L. E., Chandler, M. A., Tan, N., Contoux, C., Ramstein, G., Baatsen, M. L. J., von der Heydt, A. S., Chandan, D., Peltier, W. R., Abe-Ouchi, A., Chan, W.-L., Kamae, Y., and Brierley, C. M.: Evaluation of Arctic warming in mid-Pliocene climate simulations, Clim. Past, 16, 2325–2341, https://doi.org/10.5194/cp-16-2325-2020, 2020.

Pagani, M., Liu, Z., Lariviere, J., and Ravelo, A. C.: High Earth-system climate sensitivity determined from Pliocene carbon dioxide concentrations, Nat. Geosci. Lond., 3, 27–30, http://dx.doi.org/10.1038/ngeo724, 2010.

Pälike, H., Lyle, M. W., Nishi, H., Raffi, I., Ridgwell, A., Gamage, K., Klaus, A., Acton, G., Anderson, L., Backman, J., Baldauf, J., Beltran, C., Bohaty, S. M., Bown, P., Busch, W., Channell, J. E. T., Chun, C. O. J., Delaney, M., Dewangan, P., Dunkley Jones, T., Edgar, K. M., Evans, H., Fitch, P., Foster, G. L., Gussone, N., Hasegawa, H., Hathorne, E. C., Hayashi, H., Herrle, J. O., Holbourn, A., Hovan, S., Hyeong, K., Iijima, K., Ito, T., Kamikuri, S., Kimoto, K., Kuroda, J., Leon-Rodriguez, L., Malinverno, A., Moore Jr, T. C., Murphy, B. H., Murphy, D. P., Nakamura, H., Ogane, K., Ohneiser, C., Richter, C., Robinson, R., Rohling, E. J., Romero, O., Sawada, K., Scher, H., Schneider, L., Sluijs, A., Takata, H., Tian, J., Tsujimoto, A., Wade, B. S., Westerhold, T., Wilkens, R., Williams, T., Wilson, P. A., Yamamoto, Y., Yamamoto, S., Yamazaki, T., and Zeebe, R. E.: A Cenozoic record of the equatorial Pacific carbonate compensation depth, Nature, 488, 609–614, https://doi.org/10.1038/nature11360, 2012.

Deleted: ., Powell, R., Levy, R., Wilson, G., Scherer, R., Talarico, F., Krissek, L., Niessen, F., Pompilio, M., Wilson, T., Carter, L., DeConto, R., Huybers, P., McKay, R., Pollard, D., Ross, J., Winter, D., Barrett, P., Browne, G., Cody, R., Cowan, E., Crampton, J., Dunbar, G., Dunbar, N., Florindo, F., Gebhardt, C., Graham, I., Hannah, M., Hansaraj, D., Harwood, D., Helling, D., Henrys, S., Hinnov, L., Kuhn, G., Kyle, P., Läufer, A., Maffioli, P., Magens, D., Mandernack, K., McIntosh, W., Millan, C., Morin, R., Ohneiser, C., Paulsen, T., Persico, D., Raine, I, Reed, J., Riesselman, C., Sagnotti, L., Schmitt, D., Sjunneskog, C., Strong, P., Taviani, M., Vogel, S., Wilch, T., and Williams, T.: Obliquity-paced Pliocene West Antarctic ice sheet oscillations, Nature, 458, 322–328, https://doi.org/10.1038/nature07867, 2009.¶
Naish, T

Passchier, S.: Linkages between East Antarctic Ice Sheet extent and Southern Ocean temperatures based on a Pliocene high-resolution record of ice-rafted debris off Prydz Bay, East Antarctica, Paleoceanography, 26, https://doi.org/10.1029/2010PA002061, 2011.

1140 Peral, M., Daëron, M., Blamart, D., Bassinot, F., Dewilde, F., Smialkowski, N., Isguder, G., Bonnin, J., Jorissen, F., Kissel, C., Michel, E., Vázquez Riveiros, N., and Waelbroeck, C.: Updated calibration of the clumped isotope thermometer in planktonic and benthic foraminifera, Geochim. Cosmochim. Acta, 239, 1–16, https://doi.org/10.1016/j.gca.2018.07.016, 2018.

Piasecki, A., Bernasconi, S. M., Grauel, A.-L., Hannisdal, B., Ho, S. L., Leutert, T. J., Marchitto, T. M., Meinicke, N., Tisserand, A., and Meckler, N.: Application of Clumped Isotope Thermometry to Benthic Foraminifera, Geochem. Geophys.
1145 Geosystems, 20, 2082–2090, https://doi.org/10.1029/2018GC007961, 2019.

Rathmann, S. and Kuhnert, H.: Carbonate ion effect on Mg/Ca, Sr/Ca and stable isotopes on the benthic foraminifera Oridorsalis umbonatus off Namibia, Mar. Micropaleontol., 66, 120–133, https://doi.org/10.1016/j.marmicro.2007.08.001, 2008.

Rohling, E. J., Foster, G. L., Grant, K. M., Marino, G., Roberts, A. P., Tamisiea, M. E., and Williams, F.: Sea-level and deep-
1150 sea-temperature variability over the past 5.3 million years, Nature, 508, 477–82, http://dx.doi.org/10.1038/nature13230, 2014.

Rosenthal, Y., Perron-Cashman, S., Lear, C. H., Bard, E., Barker, S., Billups, K., Bryan, M., Delaney, M. L., deMenocal, P. B., Dwyer, G. S., Elderfield, H., German, C. R., Greaves, M., Lea, D. W., Marchitto Jr., T. M., Pak, D. K., Paradis, G. L., Russell, A. D., Schneider, R. R., Scheiderich, K., Stott, L., Tachikawa, K., Tappa, E., Thunell, R., Wara, M., Weldeab, S., and Wilson, P. A.: Interlaboratory comparison study of Mg/Ca and Sr/Ca measurements in planktonic foraminifera for
1155 paleoceanographic research, Geochem. Geophys. Geosystems, 5, https://doi.org/10.1029/2003GC000650, 2004.

Salzmann, U., Dolan, A. M., Haywood, A. M., Chan, W.-L., Voss, J., Hill, D. J., Abe-Ouchi, A., Otto-Bliesner, B., Bragg, F. J., Chandler, M. A., Contoux, C., Dowsett, H. J., Jost, A., Kamae, Y., Lohmann, G., Lunt, D. J., Pickering, S. J., Pound, M. J., Ramstein, G., Rosenbloom, N. A., Sohl, L., Stepanek, C., Ueda, H., and Zhang, Z.: Challenges in quantifying Pliocene terrestrial warming revealed by data–model discord, Nat. Clim. Change, 3, 969–974, https://doi.org/10.1038/nclimate2008,
1160 2013.

Schauble, E. A., Ghosh, P., and Eiler, J. M.: Preferential formation of 13C–18O bonds in carbonate minerals, estimated using first-principles lattice dynamics, Geochim. Cosmochim. Acta, 70, 2510–2529, https://doi.org/10.1016/j.gca.2006.02.011, 2006.

Schlitzer, Reiner, Ocean Data View (ODV 5.6.3), 2023: https://odv.awi.de/.

1165 Seki, O., Foster, G. L., Schmidt, D. N., Mackensen, A., Kawamura, K., and Pancost, R. D.: Alkenone and boron-based Pliocene pCO2 records, Earth Planet. Sci. Lett., 292, 201–211, https://doi.org/10.1016/j.epsl.2010.01.037, 2010.

Shackleton, N. J., Hall, M. A., and Boersma, A.: Oxygen and carbon isotope data from Leg 74 foraminifers, in: Initial Reports of the Deep Sea Drilling Project, vol. 74, edited by: Moore, Rabinowitz, P. D., Borelly, P., Boersma, A., and Shackleton, N. J., U.S. Government Printing Office, 599–612, https://doi.org/10.2973/dsdp.proc.74.1984, 1984.

1170 Shankle, M. G., Burls, N. J., Fedorov, A. V., Thomas, M. D., Liu, W., Penman, D. E., Ford, H. L., Jacobs, P. H., Planavsky, N. J., and Hull, P. M.: Pliocene decoupling of equatorial Pacific temperature and pH gradients, Nature, 598, 457–461, https://doi.org/10.1038/s41586-021-03884-7, 2021.

Sosdian, S. and Rosenthal, Y.: Deep-Sea Temperature and Ice Volume Changes Across the Pliocene-Pleistocene Climate Transitions, Science, 325, 306–310, https://doi.org/10.1126/science.1169938, 2009.

28

Deleted: Pollard, D. and DeConto, R. M.: Modelling West Antarctic ice sheet growth and collapse through the past five million years, Nature, 458, 329–332, https://doi.org/10.1038/nature07809, 2009.¶

Straume, E. O., Gaina, C., Medvedev, S., and Nisancioglu, K. H.: Global Cenozoic Paleobathymetry with a focus on the Northern Hemisphere Oceanic Gateways, Gondwana Res., 86, 126–143, https://doi.org/10.1016/j.gr.2020.05.011, 2020.

Thirumalai, K., Quinn, T. M., and Marino, G.: Constraining past seawater δ18O and temperature records developed from foraminiferal geochemistry, Paleoceanography, 31, 1409–1422, https://doi.org/10.1002/2016PA002970, 2016.

Tierney, J. E., Malevich, S. B., Gray, W., Vetter, L., and Thirumalai, K.: Bayesian Calibration of the Mg/Ca Paleothermometer in Planktic Foraminifera, Paleoceanogr. Paleoclimatology, 34, 2005–2030, https://doi.org/10.1029/2019PA003744, 2019.

Tripati, A. K., Eagle, R. A., Thiagarajan, N., Gagnon, A. C., Bauch, H., Halloran, P. R., and Eiler, J. M.: 13C–18O isotope signatures and 'clumped isotope' thermometry in foraminifera and coccoliths, Geochim. Cosmochim. Acta, 74, 5697–5717, https://doi.org/10.1016/j.gca.2010.07.006, 2010.

de la Vega, E., Chalk, T. B., Wilson, P. A., Bysani, R. P., and Foster, G. L.: Atmospheric CO2 during the Mid-Piacenzian Warm Period and the M2 glaciation, Sci. Rep., 10, 11002, https://doi.org/10.1038/s41598-020-67154-8, 2020.

Wara, M. W., Ravelo, A. C., and Delaney, M. L.: Permanent El Niño-Like Conditions During the Pliocene Warm Period, Science, 309, 758–761, https://doi.org/10.1126/science.1112596, 2005.

Weiffenbach, J. E., Baatsen, M. L. J., Dijkstra, H. A., von der Heydt, A. S., Abe-Ouchi, A., Brady, E. C., Chan, W.-L., Chandan, D., Chandler, M. A., Contoux, C., Feng, R., Guo, C., Han, Z., Haywood, A. M., Li, Q., Li, X., Lohmann, G., Lunt, D. J., Nisancioglu, K. H., Otto-Bliesner, B. L., Peltier, W. R., Ramstein, G., Sohl, L. E., Stepanek, C., Tan, N., Tindall, J. C., Williams, C. J. R., Zhang, Q., and Zhang, Z.: Unraveling the mechanisms and implications of a stronger mid-Pliocene Atlantic Meridional Overturning Circulation (AMOC) in PlioMIP2, Clim. Past, 19, 61–85, https://doi.org/10.5194/cp-19-61-2023, 2023.

Wilkinson, B. H. and Algeo, T. J.: Sedimentary carbonate record of calcium-magnesium cycling, Am. J. Sci., 289, 1158–1194, https://doi.org/10.2475/ajs.289.10.1158, 1989.

Woodard, S. C., Rosenthal, Y., Miller, K. G., Wright, J. D., Chiu, B. K., and Lawrence, K. T.: Antarctic role in Northern Hemisphere glaciation, Science, 346, 847–851, https://doi.org/10.1126/science.1255586, 2014.

Yu, J. and Broecker, W. S.: Comment on "Deep-Sea Temperature and Ice Volume Changes Across the Pliocene-Pleistocene Climate Transitions," Science, 328, 1480–1480, https://doi.org/10.1126/science.1186544, 2010.